Spectroscopy and Imaging of Edge Modes in Permalloy Nanodisks

Feng Guo*

Center for Nanoscale Science and Technology, National Institute of Standards and Technology, Gaithersburg, Maryland 20899, USA and Maryland Nanocenter, University of Maryland, College Park, Maryland 20742, USA

L. M. Belova

Department of Materials Science and Engineering, Royal Institute of Technology, 10044 Stockholm, Sweden

R. D. McMichael†

Center for Nanoscale Science and Technology, National Institute of Standards and Technology, Gaithersburg, Maryland 20899, USA

(Received 24 August 2012; published 3 January 2013)

We report ferromagnetic resonance force microscopy of confined spin-wave modes with improved, 100 nm resolution. The ferromagnetic resonance spectra in Permalloy disks (diameters ranging from 100 to 750 nm) distinguish multiple edge modes, and the images reveal distinct precession patterns. The fundamental edge mode also provides a new, localized probe of the magnetic properties of the film edge; rotation of the applied field reveals large edge property variations in nominally circular disks. As a function of disk diameter, the number of observed edge modes agrees with modeling.

DOI: 10.1103/PhysRevLett.110.017601 PACS numbers: 76.50.+g, 68.37.Rt, 75.30.Ds, 75.75.Jn

Magnetic nanostructures are building blocks for novel magnetic memory devices, and the magnetic properties change remarkably when the size of the magnetic structures reduces into nanometer range. In particular, a simple geometrical argument suggests that the properties of the edges become relatively more important with decreasing size. Therefore, edge related effects in ferromagnetic nanostructures become a major area of interest for both fundamental physics and for applications. Here, we present a study of the spectroscopy and imaging of magnetic edge modes, with a great improvement in spatially resolving mode profiles. We also introduce a new method to measure inhomogeneity in edge properties along the edge of a single structure.

The strong inhomogeneity in the internal magnetic field at the edges of a film allows spin waves to be localized in these regions [1–5], and the localization allows the trapped-spin-wave "edge modes" to serve as sensitive probes of the magnetic properties of the film edge. The edge properties have been intensively studied [6–16] both experimentally and theoretically, including the effects of sidewall angle [10], intralayer interactions [12], influence of the oxidation [11], structure size and shape [13–15], and film thickness [13,16]. In a majority of these studies, the net response of a large array of nanostructures is measured, and the measurements represent the average properties over the large number of structures and/or edges in the array.

Over the past decade, several techniques have been successfully developed that spatially resolved magnetization dynamics at GHz frequencies. These methods include time resolved Kerr microscopy [2,5] and microfocus Brillouin light scattering spectroscopy, where a spatial resolution of 250 nm has been reported [9]. A very challenging variation is near-field Brillouin scattering, which has been used to image edge mode dynamics with resolution below 55 nm [17]. X-ray microscopy based on magnetic circular dichroism also provides dynamic magnetic imaging [18–20] with resolution as fine as 25 nm [18].

In parallel, ferromagnetic resonance force microscopy (FMRFM) [21–24] has been developed and proven to be a useful tool for various areas in magnetic dynamics, such as spin-wave dynamics in confined structures [22,25–30], spin-transfer torque device dynamics [31], defect detection in an array [32], and spin-wave localization [33–36]. With spin waves localized by the stray field from the FMRFM tip, a resolution of 200 nm has been reported [33].

In this Letter, we begin with an introduction to the precession modes in a nanodisk as predicted by micromagnetic modeling. We then describe FMRFM spectroscopy and imaging of trapped-spin-wave edge modes with a resolution of 100 nm. Using the same measurement scheme, we demonstrate an approach to detect the edge properties along the disk edge. Finally, we discuss the disk size dependence of the edge mode spectra.

Micromagnetic modeling [37] results shown in Fig. 1 introduce a few of the normal modes of an in-plane magnetized disk. The susceptibility spectrum and precession mode profiles are shown for a 500 nm diameter, 25 nm thick disk with Permalloy (Py) material parameters [38] and a static external field applied in-plane. The modes are excited with a uniform 10 GHz transverse field, and the four highest intensity modes are shown in the spectrum in Fig. 1(a). From the spatial profiles of these modes [insets of Figs. 1(a) and 1(b)], it is clear that the three weaker modes

 © 2013 American Physical Society

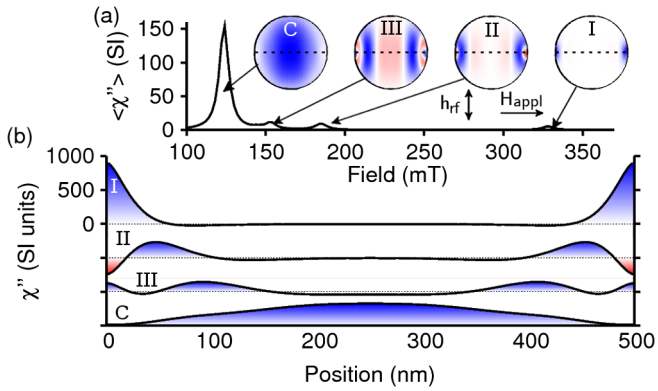

FIG. 1 (color online). (a) Micromagnetic modeling of the spectrum calculated for a 500 nm disk with a 10 GHz uniform driving field. The static field is applied parallel to the dotted lines in the insets. (b) Modeled spatial profiles of the imaginary part of the susceptibility for various modes. The shading in (b) is the color scale for the insets in (a).

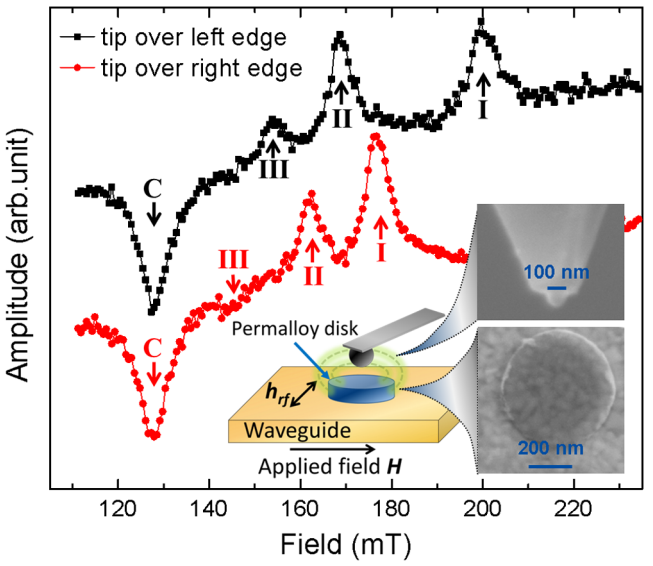

FIG. 2 (color online). Measured spectra when the tip is over the left edge (upper spectrum) and right edge (lower spectrum) of a nominally 500 nm diameter disk. The microwave frequency used for this measurement is 10 GHz. The vertical offset is applied for clarity. The insets show a conceptual sketch of the experimental setup and scanning electron microscope images of the cantilever tip with cobalt hemisphere and the disk with diameters of 530 and 545 nm in the x and y directions.

feature precession localized near the edges [3]. The mode with the largest precession at the very edge (I) has the highest resonance field. Two other edge modes (II and III) have lower resonance fields and precession maxima located further away from the edge. The main mode near 120 mT (C) features precession across almost the whole disk, with maximum amplitude at the center.

Experimentally, the FMRFM measurements use precession-induced changes to the dipole-dipole forces between the sample and a magnetic cantilever tip to detect precession modes in the sample. The schematic of the setup is shown in the inset of Fig. 2. The samples consist of Ta(5 nm)/Py(25 nm)/Ta(5 nm) layers deposited by electron-beam evaporation onto a rotating substrate; they are patterned into circular disks using electron-beam lithography and a lift-off technique. The samples are deposited on a 2 μm wide center stripe of a coplanar waveguide that is made of 150 nm thick gold.

A quasistatic field aligns the sample magnetization in the plane of the sample, and microwave current in the waveguide generates a rf magnetic field that drives magnetization precession. We modulate the microwave power (and, accordingly, the rf field, precession amplitude, quasistatic magnetization of the sample, and tip-sample dipole force) at the mechanical vibration frequency of the cantilever (typically 8 kHz, $Q \approx 1000$) for lock-in signal detection. The square of the precession amplitude is thus measured via the cantilever oscillation amplitude [22].

A 100 nm diameter roughly hemispherical tip of cobalt is used in this study. The tip was fabricated through electron-beam-induced deposition [39], and a scanning electron microscope image of the tip is shown in the inset of Fig. 2. In contrast to some of the previous work [33–36] where the spin waves in the films were localized by the strong tip fields, this tip has a much weaker stray field due to its small size and no tip-localized modes have been observed. The tip is typically lifted 50 nm off of the sample surface. All measurements are done in vacuum at ambient temperature.

The resonance spectra are obtained by exciting the sample at a given microwave frequency and sweeping the in-plane magnetic field while recording the cantilever oscillation. Figure 2 shows two spectra measured when the tip is positioned above either the left or right edge of a 500 nm diameter disk with the applied field directed from left to right. These spectra show quantitatively similar results with one negative-going resonance around 130 mT and several peaks at higher field. In contrast to the symmetric profiles predicted by the micromagnetic model, these measured high field resonances occur at different field values for different edges, probably due to the nonideal, inhomogeneous edges resulted from the lift-off process [6,10,11,13–16].

To further investigate the nature of the measured modes, the 1D position dependence of the spectra is measured as the tip moves across the disk, shown in Fig. 3(a). When the tip is close to the left edge, three modes (with resonances 154, 167, and 198 mT) are found to have maximum intensities and they rapidly weaken as the tip moves away from the left edge. Similarly, there are also several different modes that are observed only in the vicinity of the right edge. Consistent with the spectra in Fig. 2, the modes at the right edge show distinctly different resonance fields from those at the left edge, particularly the highest field mode. Since all these modes are localized near the edges of the

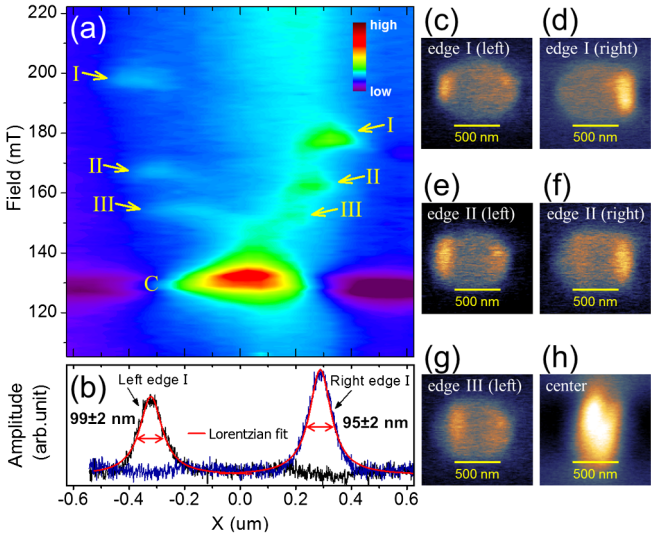

FIG. 3 (color online). (a) 1D spectroscopic scan measured via moving the tip across the 500 nm disk with 10 GHz excitation frequency. (b) 1D spatial profiles for left and right edge I modes after background subtraction. (c)–(h) 2D imaging for the left edge I, right edge I, left edge II, right edge II, left edge III, and center modes, respectively.

disk, we label them as edge modes (edge I, edge II, and edge III with decreasing resonant fields). The mode around 130 mT has maximum positive signal when the tip is near the disk center; thus, we refer to it as the center mode. When the tip is moved outside of the disk, the center mode yields negative signal as the tip-sample interaction becomes attractive, indicated by the dark (purple and black) areas in Fig. 3(a). The small change in resonance field of the center mode when the tip moves off of the sample indicates a small stray field from the tip [30,40].

A subtler effect is that, for the decreasing series of resonance fields in Fig. 3(a), the spatial positions of the edge mode resonances progress inward from the edge of the disk, and this behavior is in accord with the behavior of the modeled precession profiles plotted in Fig. 1(b).

In order to measure the spatial profiles of these modes, we perform 1D spatial scans. The magnetic field is fixed at the resonance of the mode of interest when FMRFM signal is measured as a function of the tip position along a line bisecting the disk. Figure 3(b) shows examples for 1D line scans of edge I modes for both left and right edges. Here, a background signal taken at an off-resonance field has been subtracted. We find that the scans are well fit by Lorentzians with full widths of about 100 nm, providing an upper bound for the spatial resolution.

With the applied field held at a resonance field, the tip is scanned to obtain 2D mode images such as those shown in Figs. 3(c)–3(h). The edge mode images have a radial width on the order of 100 nm but have much wider distribution in the tangential direction. This elongated image shape is partly due to the elongated shape of edge mode profiles [Fig. 1(a)], but additionally, the point response function for the in-plane magnetized tip yields images that appear elongated in the same direction [36]. In addition to contrast from the modes of interest, a faint frequency- or field-independent background signal with the shape of the disk can be seen in the 2D images. We speculate that this background results from thermal modulation of the sample magnetization by the microwave power.

Unlike the symmetric edge behavior predicted by the modeling, there are differences between the measured spectra for the left and right edges, as exemplified in Fig. 2. These differences might be attributable to the changes in the edge properties (side wall angle, oxidation, etc.) from one side of the disk to the other, and that possibility raises the question of how the edge properties vary along the disk edges. In order to measure edge property variations, the applied magnetic field is rotated away from the waveguide direction but still maintained in the plane. Figures 4(a) and 4(b) show the 2D spatial imaging of the edge I mode in the 500 nm disk when the field is directed along the waveguide at 0° and at 30° from the waveguide axis. These images show that the edge modes follow the field orientation.

The angular dependences of the resonances are shown in Fig. 4(c). For each applied field angle, the tip is moved to the corresponding edge position in order to measure the edge spectrum, and the procedure is repeated to trace along the entire disk edge. The edge I mode's resonance field, especially, shows a rather large angular dependence, suggesting that the edge I mode is the most sensitive to the local property of the edge. By contrast, the other two edge modes, being slightly away from the edge, have relatively less dependence on the angle. The center mode is effectively independent of the field angle [14]. For comparison,

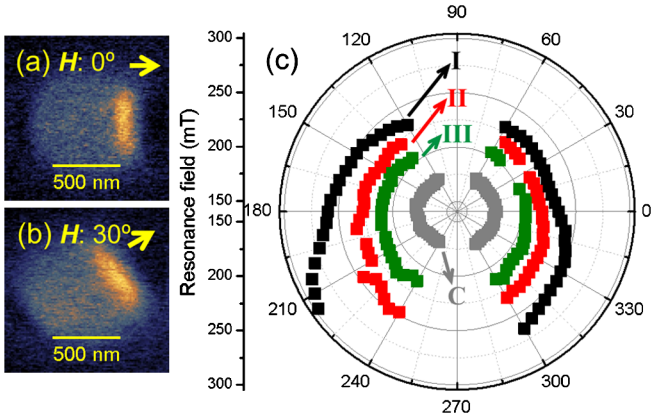

FIG. 4 (color online). 2D imaging of the right edge modes in the 500 nm disk. (a) The applied field aligns with the length of the waveguide. (b) The applied field is 30° off the length of the waveguide. (c) Resonances of center and edge modes as functions of the applied field angle with 12 GHz microwave frequency. The error bar is smaller than the size of the symbols.

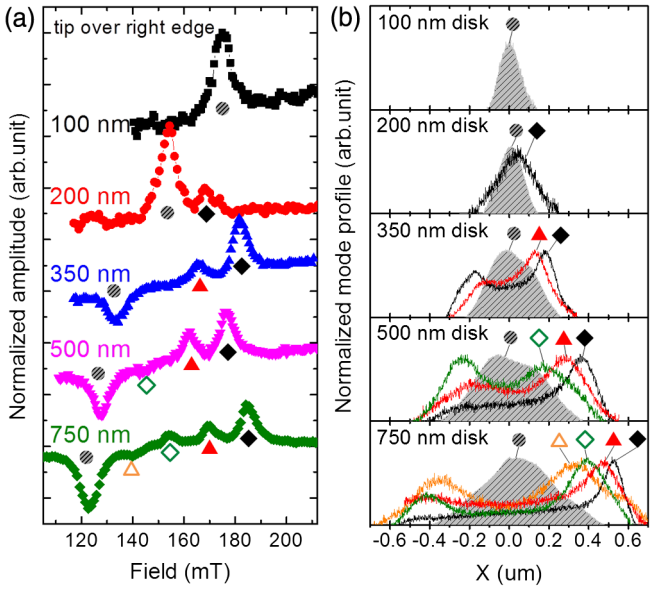

FIG. 5 (color online). (a) Measured spectra of the right edges for 100, 200, 350, 500, and 750 nm disks with 10 GHz excitation frequency. (b) 1D spatial mode profiles measured in the same disks as those in (a). The colors of the modes match the marks labeled in (a).

typical standard deviations of the fit resonance fields are approximately 1 mT. Note that no spectra are recorded near 90° and 270° where the applied field is nearly parallel to the rf magnetic field, resulting in very low effective pumping power.

So far, we have only discussed the properties of the edge modes in the 500 nm diameter disk, and we now turn to the dependence of the edge modes on disk diameter. Figure 5(a) shows measured spectra when the tip is positioned above the right edges of disks with diameters ranging from 100 to 750 nm. Note that, for the measured modes, both the sign and the peak intensity depend on the tip position [Fig. 3(a)]. The modes' resonance fields, however, are nearly independent of tip position, indicating a weak tip field. The center mode is observed in all the disks, and edge modes are observed in all of the samples except for the 100 nm disk. The number of edge modes depends on the disk size, with generally more edge modes appearing in larger disks, as summarized in Table I. 1D FMRFM line scans, with the applied fields fixed at the right edge resonances in Fig. 5(a), are also plotted in Fig. 5(b) to illustrate the relative spatial distributions for different edge modes.

The size-dependent behavior of the edge modes is largely reproduced by the micromagnetic model that includes stray fields from a magnetically soft tip 100 nm in diameter and 50 nm above the sample. Figure 6 shows simulated signals as functions of tip position for different modes and for different disk sizes. The number of distinct edge mode resonances is compared with the measurement in Table I. Despite clear differences between the modeled and measured resonance fields of the edge I modes (Fig. 2), measurement and modeling show close agreement on the number of distinct edge mode resonances over a range of disk diameters.

TABLE I. Number of edge modes measured or modeled for different disk diameters. The measured modes are observed with 10 GHz excitation, and the modeled modes are calculated at an applied field of 0.15 T.

Diameter (nm)	100	200	350	500	750
Measurement	0	1	1	2	4
Model	1	1	2	3	5

In summary, we have used ferromagnetic resonance force microscopy to probe magnetization dynamics in magnetic nanostructures with 100 nm resolution. The improvement in resolution opens doors to magnetic characterization for a variety of spintronic device schemes. In disks, we have presented both spectra and images of multiple spin-wave modes near the edges of ferromagnetic nanostructures. Each edge mode not only has a specific resonance but also has a distinct location of maximum precession amplitude relative to the edge. We have also used the edge modes as local probes of edge properties, revealing magnetic inhomogeneity along the film edge. The sample size dependence study shows that the number of edge modes decreases with decreasing disk size.

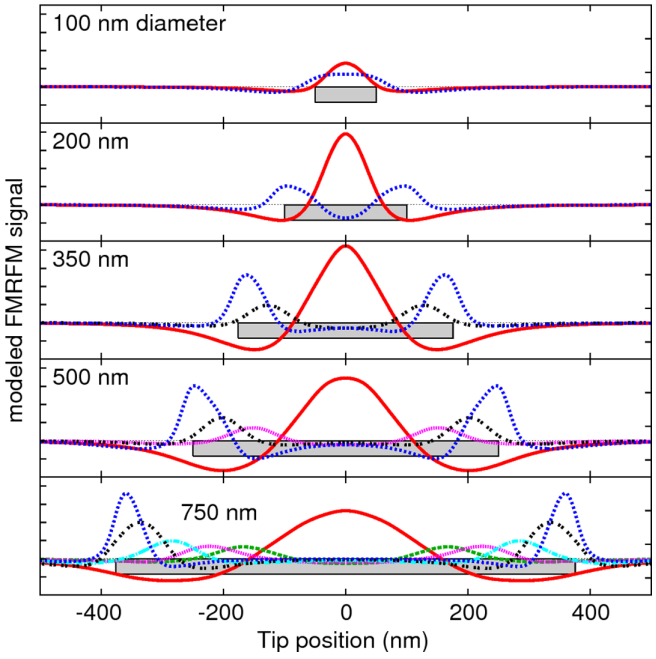

FIG. 6 (color online). Modeled FMRFM tip force for the center (solid curves) and edge (dotted curves) modes (from top to bottom) in 100, 200, 350, 500, and 750 nm diameter disks, each with an applied field of 0.15 T.

The authors thank Dr. Han Jong Chia for helpful discussions. Dr. Guo acknowledges support under the Cooperative Research Agreement between the University of Maryland and the National Institute of Standards and Technology Center for Nanoscale Science and Technology, Award No. 70NANB10H193, through the University of Maryland. Dr. Belova acknowledges support from the Swedish Research Council and the Swedish Innovation Agency VINNOVA.

*feng.guo@nist.gov
†robert.mcmichael@nist.gov

[1] J. Jorzick, S. O. Demokritov, B. Hillebrands, M. Bailleul, C. Fermon, K. Y. Guslienko, A. N. Slavin, D. V. Berkov, and N. L. Gorn, Phys. Rev. Lett. **88**, 047204 (2002).
[2] J. P. Park, P. Eames, D. M. Engebretson, J. Berezovsky, and P. A. Crowell, Phys. Rev. Lett. **89**, 277201 (2002).
[3] C. Bayer, S. O. Demokritov, B. Hillebrands, and A. N. Slavin, Appl. Phys. Lett. **82**, 607 (2003).
[4] M. Bailleul, D. Olligs, and C. Fermon, Phys. Rev. Lett. **91**, 137204 (2003).
[5] C. Bayer, J. P. Park, H. Wang, M. Yan, C. E. Campbell, and P. A. Crowell, Phys. Rev. B **69**, 134401 (2004).
[6] R. D. McMichael and B. B. Maranville, Phys. Rev. B **74**, 024424 (2006).
[7] B. B. Maranville, R. D. McMichael, S. A. Kim, W. L. Johnson, C. A. Ross, and J. Y. Cheng, J. Appl. Phys. **99**, 08C703 (2006).
[8] V. V. Kruglyak, P. S. Keatley, R. J. Hicken, J. R. Childress, and J. A. Katine, J. Appl. Phys. **99**, 08F306 (2006).
[9] V. E. Demidov, M. Buchmeier, K. Rott, P. Krzysteczko, J. Münchenberger, G. Reiss, and S. O. Demokritov, Phys. Rev. Lett. **104**, 217203 (2010).
[10] B. B. Maranville, R. D. McMichael, and D. W. Abraham, Appl. Phys. Lett. **90**, 232504 (2007).
[11] M. Zhu and R. D. McMichael, J. Appl. Phys. **107**, 103908 (2010).
[12] M. Zhu and R. D. McMichael, J. Appl. Phys. **109**, 043904 (2011).
[13] J. M. Shaw, T. J. Silva, M. L. Schneider, and R. D. McMichael, Phys. Rev. B **79**, 184404 (2009).
[14] H. T. Nembach, J. M. Shaw, T. J. Silva, W. L. Johnson, S. A. Kim, R. D. McMichael, and P. Kabos, Phys. Rev. B **83**, 094427 (2011).
[15] V. V. Kruglyak, A. Barman, R. J. Hicken, J. R. Childress, and J. A. Katine, Phys. Rev. B **71**, 220409 (2005).
[16] R. D. McMichael, C. A. Ross, and V. P. Chuang, J. Appl. Phys. **103**, 07C505 (2008).
[17] J. Jersch, V. E. Demidov, H. Fuchs, K. Rott, P. Krzysteczko, J. Münchenberger, G. Reiss, and S. O. Demokritov, Appl. Phys. Lett. **97**, 152502 (2010).
[18] B. L. Mesler, K. S. Buchanan, M.-Y. Im, and P. Fischer, J. Appl. Phys. **111**, 07D311 (2012).
[19] H. H. Langner, T. Kamionka, M. Martens, M. Weigand, C. F. Adolff, U. Merkt, and G. Meier, Phys. Rev. B **85**, 174436 (2012).
[20] A. Vogel, T. Kamionka, M. Martens, A. Drews, K. W. Chou, T. Tyliszczak, H. Stoll, B. Van Waeyenberge, and G. Meier, Phys. Rev. Lett. **106**, 137201 (2011).
[21] Z. Zhang, P. C. Hammel, and P. E. Wigen, Appl. Phys. Lett. **68**, 2005 (1996).
[22] O. Klein, G. de Loubens, V. V. Naletov, F. Boust, T. Guillet, H. Hurdequint, A. Leksikov, A. N. Slavin, V. S. Tiberkevich, and N. Vukadinovic, Phys. Rev. B **78**, 144410 (2008).
[23] P. C. Hammel and D. V. Pelekhov, in *Handbook of Magnetism and Advanced Magnetic Materials* (Wiley, New York, 2007), Vol. 5.
[24] M. M. Midzor, P. E. Wigen, D. Pelekhov, W. Chen, P. C. Hammel, and M. L. Roukes, J. Appl. Phys. **87**, 6493 (2000).
[25] Y. Obukhov, D. V. Pelekhov, J. Kim, P. Banerjee, I. Martin, E. Nazaretski, R. Movshovich, S. An, T. J. Gramila, S. Batra *et al.*, Phys. Rev. Lett. **100**, 197601 (2008).
[26] R. Urban, A. Putilin, P. E. Wigen, S.-H. Liou, M. C. Cross, P. C. Hammel, and M. L. Roukes, Phys. Rev. B **73**, 212410 (2006).
[27] T. Mewes, J. Kim, D. V. Pelekhov, G. N. Kakazei, P. E. Wigen, S. Batra, and P. C. Hammel, Phys. Rev. B **74**, 144424 (2006).
[28] G. de Loubens, A. Riegler, B. Pigeau, F. Lochner, F. Boust, K. Y. Guslienko, H. Hurdequint, L. W. Molenkamp, G. Schmidt, A. N. Slavin *et al.*, Phys. Rev. Lett. **102**, 177602 (2009).
[29] G. de Loubens, V. V. Naletov, O. Klein, J. B. Youssef, F. Boust, and N. Vukadinovic, Phys. Rev. Lett. **98**, 127601 (2007).
[30] H.-J. Chia, F. Guo, L. M. Belova, and R. D. McMichael, Appl. Phys. Lett. **101**, 042408 (2012).
[31] A. Hamadeh, G. de Loubens, V. V. Naletov, J. Grollier, C. Ulysse, V. Cros, and O. Klein, Phys. Rev. B **85**, 140408 (2012).
[32] H.-J. Chia, F. Guo, L. M. Belova, and R. D. McMichael, Phys. Rev. B **86**, 184406 (2012).
[33] I. Lee, Y. Obukhov, G. Xiang, A. Hauser, F. Yang, P. Banerjee, D. Pelekhov, and P. Hammel, Nature (London) **466**, 845 (2010).
[34] I. Lee, Y. Obukhov, A. J. Hauser, F. Y. Yang, D. V. Pelekhov, and P. C. Hammel, J. Appl. Phys. **109**, 07D313 (2011).
[35] E. Nazaretski, D. V. Pelekhov, I. Martin, M. Zalalutdinov, D. Ponarin, A. Smirnov, P. C. Hammel, and R. Movshovich, Phys. Rev. B **79**, 132401 (2009).
[36] H.-J. Chia, F. Guo, L. M. Belova, and R. D. McMichael, Phys. Rev. Lett. **108**, 087206 (2012).
[37] M. J. Donahue and D. G. Porter, in National Institute of Standards and Technology Interagency Report No. NISTIR 6376, 1999.
[38] Magnetization $M = 800$ kA/m, exchange stiffness 13 pJ/m, Gilbert damping $\alpha_G = 0.01$.
[39] L. M. Belova, E. D. Dahlberg, A. Riazanova, J. J. L. Mulders, C. Christophersen, and J. Eckert, Nanotechnology **22**, 145305 (2011).
[40] From the shift of resonance field between attractive and repulsive regions, the tip field is estimated to be on the order of 5 mT, a value that is consistent with a separation experiment on the tip's lift-off height dependence.